Report No. 169 / UILU ENG-95-4001

$^{e}\sigma$ and $^{e}\varepsilon$ Based Approaches to Multiaxial Notch Analysis

by

Volker B. Köttgen, Mark E. Barkey and Darrell F. Socie

A report of
MATERIALS ENGINEERING — MECHANICAL BEHAVIOR
College of Engineering, University of Illinois at Urbana-Champaign
January 1995

${}^e\sigma$ and ${}^e\varepsilon$ based approaches to multiaxial notch analysis

Volker B. Köttgen
TecMath GmbH, Sauerwiesen 2, D-67661 Kaiserslautern, FRG
formerly at Technische Hochschule Darmstadt,
Fachgebiet Werkstoffmechanik

Mark E. Barkey
and
Darrell F. Socie
University of Illinois at Urbana-Champaign,
Department of Mechanical and Industrial Engineering,
1206 West Green Street, Urbana, IL 61801, USA

January, 1995
submitted to
Fatigue and Fracture of Engineering Materials and Structures

The analysis of notch stresses and strains is one of the key parts of fatigue life prediction of components and structures. In this paper two related approaches are introduced, covering the whole field from uniaxial to multiaxial non-proportional loading. The stress at the notch root computed by theory of elasticity, ${}^e\sigma$, is introduced as the governing variable for elastic-plastic notch analysis. Although ${}^e\sigma$ is just a specially defined nominal stress, it eases notch analysis in comparison to using arbitrarily definable nominal stresses, especially for non-proportional multiaxial loading. Additionally an ${}^e\varepsilon$ (strain) based approach is introduced and compared to the ${}^e\sigma$ approach. Both proportional and non-proportional loading are discussed, and compared to the approaches by HOFFMANN and SEEGER and by BARKEY *et al.*.

LIST OF SYMBOLS

c	–	dimensional proportionality constant relating local structural response to loading, similar to K_t
e	–	subscript denoting the elastic part of a quantity
E	–	YOUNG's modulus
ε	–	local (notch) strain
${}^{e}\varepsilon$	–	fictitious local strain computed by theory of elasticity
$f({}^{e}\sigma)$, $\mathcal{F}$	–	load-notch strain curves
f_0	–	criterion for the onset of yielding
F_0, G_0, H_0	–	coefficients of HILL's yield criterion
$g(\sigma)$	–	stress-strain curve
γ	–	shear strain
H'	–	work-hardening modulus of an equivalent stress vs. equivalent plastic strain curve
K_t	–	(nondimensional) stress concentration factor
L	–	load (force, moment, displacement, etc.)
L_0	–	load at the start of yielding
L_p	–	fully plastic limit load (elastic-perfectly plastic material)
m	–	counter for different load components
M_0, N_0, O_0	–	coefficients of HILL's yield criterion
n	–	number of different load components
ν	–	POISSON's ratio

p	–	Subscript denoting the plastic part of a quantity
q	–	subscript denoting an equivalent quantity, e.g. VON MISES equivalent stress
S	–	nominal stress
s	–	deviatoric part of a stress tensor $s_{ij} = \sigma_{ij} - \bar{\sigma}$
σ	–	local (notch) stress
${}^{e}\sigma$	–	fictitious local stress computed by theory of elasticity
σ_U	–	yield stress
$\bar{\sigma}$	–	hydrostatic pressure $\bar{\sigma} = \frac{1}{3}\sigma_{kk}$
τ	–	shear stress
x, y, z	–	local cartesian coordinates
X, Y, Z	–	global cartesian coordiantes (for nominal stresses)

1 NOMINAL STRESSES AND ${}^e\sigma$

Commonly in fatigue analysis, the 'loading' is expressed in terms of nominal stresses S, which can be arbitrarily defined as long as they are proportional to the exterior loading. Often nominal stresses are defined as stresses in the net section of the component computed by elementary mechanics. Local stresses can be computed from nominal stresses via non-dimensional stress concentration factors K_t. Nominal stresses and stress concentration factors constitute pairs of variables, i.e. one may not be redefined without changing the other accordingly, because the real governing variable is the stress at the notch root computed by linear theory of elasticity

$$ {}^e\sigma = K_t \cdot S. \tag{1} $$

For more complex components and for multiaxial loading the definition of a 'net section' is often not trivial. More than that: it is also not required, because implicitly or explicitly ${}^e\sigma$ will have to be used anyway. Considering a structure loaded by n different 'loads' L (forces, or moments, displacements, etc.), the stress tensor ${}^e\sigma_{ij}$ at any structural location computed by theory of elasticity can be expressed by

$$ {}^e\sigma_{ij} = \sum_{m=1}^{n} (c_{ij})_m \cdot L_m = \sum_{m=1}^{n} (K_{t,ij})_m \cdot S_m, \tag{2} $$

where c_{ij} are dimensional proportionality constants. Like any nominal stress the stress tensor ${}^e\sigma$ is fictitious[1] for the elastic-plastic notch root behaviour that has to be considered in fatigue.

For uniaxial loading this elastic-plastic behaviour is often approximated using an estimation formula. Although these formulas are usually written

[1] the left-hand superscript e is used to avoid confusion with the subscript e denoting the elastic part of a real, i.e. measurable, quantity like the elastic strain tensor $\varepsilon_{e,ij}$. In this paper ${}^e\sigma$ will be called 'pseudo stress', and ${}^e\varepsilon$ 'pseudo strain'.

in terms of nominal stresses, they can be rewritten in terms of ${}^{e}\sigma$. This can be seen for NEUBER's rule below fully plastic yielding

$$\sigma \cdot \varepsilon = K_\varepsilon \cdot K_\sigma = \frac{(K_t \cdot S)^2}{E} = \frac{({}^{e}\sigma)^2}{E} \tag{3}$$

$$\varepsilon = g(\sigma) \tag{4}$$

but even the generalization of this formula suggested by SEEGER and HEULER [1] can be written in terms of ${}^{e}\sigma$

$$\sigma \cdot \varepsilon = \frac{({}^{e}\sigma)^2}{E} \cdot \left(\frac{e^* \cdot E}{S^*} \right) \tag{5}$$

$$S^* = {}^{e}\sigma \cdot \frac{L_p}{L_0} \tag{6}$$

$$\varepsilon = g(\sigma) \tag{7}$$

$$\varepsilon^* = g(S^*) \tag{8}$$

only the ratio between the load at the fully plastic limit state L_p and the load at the start of yielding L_0 has to be introduced as an additional variable.

2 YIELD SURFACE AT THE NOTCH

Unlike a nominal stress, ${}^{e}\sigma$ can be used immediately to compute the onset of yielding. Assuming validity of the isotropic VON MISES yield criterion for the *material*, yielding then starts at

$$f_0({}^{e}\sigma_{ij}) = 0.5 \left[({}^{e}\sigma_x - {}^{e}\sigma_y)^2 + ({}^{e}\sigma_y - {}^{e}\sigma_z)^2 + ({}^{e}\sigma_z - {}^{e}\sigma_x)^2 \right] + 3 \left({}^{e}\tau_{xy}^2 + {}^{e}\tau_{yz}^2 + {}^{e}\tau_{zx}^2 \right) = \sigma_0^2, \tag{9}$$

where σ_0 is the uniaxial yield stress. At the surface of the specimen ${}^{e}\sigma_y$, ${}^{e}\tau_{xy}$ and ${}^{e}\tau_{yz}$ may be zero depending on the local tractions.

Re-arranging Eq. (9) with Eq. (2) yielding can be expressed in terms of

the n different loads L_m acting on the structure

$$\begin{aligned} f_0(L) &= \sum_{m=1}^{n} \Big[0.5 \left((c_{x,m} - c_{y,m})^2 + (c_{y,m} - c_{z,m})^2 + (c_{z,m} - c_{x,m})^2 \right) + \\ &\qquad 3 \left(c_{xy,m}^2 + c_{yz,m}^2 + c_{zx,m}^2 \right) \Big] \cdot L_m^2 + \\ &\quad \sum_{k=1}^{n-1} \sum_{l=k+1}^{n} \Big[(c_{x,k} - c_{y,k}) \cdot (c_{x,l} - c_{y,l}) + (c_{y,k} - c_{z,k}) \cdot (c_{y,l} - c_{z,l}) + \\ &\qquad (c_{z,k} - c_{x,k}) \cdot (c_{z,l} - c_{x,l}) + \\ &\qquad 6 \left(c_{xy,k} \cdot c_{xy,l} + c_{yz,k} \cdot c_{yz,l} + c_{zx,k} \cdot c_{zx,l} \right) \Big] \cdot L_k \cdot L_l \\ &= \sigma_0^2. \end{aligned} \tag{10}$$

Specializing Eq. (10) for a notched round bar as sketched in Fig. 1, where an axial nominal stress S_Z leads only to axial and transverse stresses σ_z, σ_x at the notch root and where a torsional nominal stress S_{XZ} produces only local shear stresses τ_{xz}, gives

$$f_0(S_Z, S_{XZ}) = \left(K_{t,z}^2 - K_{t,z} \cdot K_{t,x} + K_{t,x}^2 \right) \cdot S_Z^2 + 3 \, K_{t,xz}^2 \cdot S_{XZ}^2 = \sigma_0^2. \tag{11}$$

Here X and Z denote the coordinate system for nominal stresses, and x, z the local coordinate system at the notch root as sketched in Fig. 1. The local circumferential stress caused by the axial nominal stress is ${}^e\sigma_x = K_{t,x} \cdot S_Z$.

In [2, 3] BARKEY *et al.* have proposed a multiaxial notch analysis approach using an *anisotropic structural* yield surface defined in terms of *nominal stresses*, which was written for the general case using HILL's yield criterion as

$$\begin{aligned} 2 \, f_0(S_{ij}) &= F_0 \, (S_X - S_Y)^2 + G_0 \, (S_Y - S_Z)^2 + H_0 \, (S_Z - S_X)^2 + \\ &\qquad 2M_0 \, S_{XY}^2 + 2N_0 \, S_{YZ}^2 + 2O_0 \, S_{ZX}^2 = 1. \end{aligned} \tag{12}$$

The coefficients F_0, G_0, H_0, M_0, N_0, O_0 have to be determined by computing the onset of yielding at the notch root for individually applied nominal stress

components. In spite of the formulation in nominal stresses and the name 'structural yield surface', Eq. (12) really describes a 'local' or 'notch yield surface', which differs for every structural location in a given component.

The mathematical nature of HILL's yield criterion imposes certain restrictions on the type of loading which may be analyzed. Most importantly, elastic coupling at the notch root between any two nominal stresses is not allowed. This can be seen by comparing the coefficients of Eq. (10) and Eq. (12): If a certain local stress component is activated by more than one external load, the mixed terms $L_k \cdot L_l$ (or $S_{ij} \cdot S_{jk}$, respectively) present in Eq. (10) are missing in the anisotropic structural yield surface based on HILL's criterion Eq. (12).

Such cases occur, e.g., for combined bending and axial loading of the notched round bar at the notch surface or when locations in the interior of a component are analysed, which may be potential crack initiation sites under non-proportional loading or when they have different fatigue properties than points on the surface. While decoupling of normal and shear components is possible by transforming nominal stresses into a coordinate system corresponding to a local principal stress system (for ${}^e\sigma_{ij}$), decoupling between axial and bending loads is not possible using HILL's criterion. For the case of the notched round bar, however, Eq. (11) can be obtained from the general approach of Eq. (12). Thus, the *isotropic*, ${}^e\sigma$ based yield criterion of Eq. (9) is easier to use and somewhat more general than the *anisotropic structural* yield surface originally proposed in [2, 3], but the basic idea of both approaches is the same.

3 MODELLING MATERIAL DEFORMATION BEHAVIOUR

Obviously, the stress-strain response at the *notch* is influenced strongly by the deformation behaviour of the *material*. Thus, a model for notch response can either be valid for one particular material model only, or it can be a general framework accommodating many material models. The latter approach is used in this paper. It is, however, inevitable to discuss some basic features of material models, because they will be reflected by the notch model, too.

For fatigue life prediction under uniaxial loading there is a broad consensus that modelling stabilized stress-strain response is sufficiently accurate in most cases. The model describing this behaviour is characterized by MASING's hypothesis [5] and Rainflow-type memory rules [6, 7].

In spite of intensive research on material models for multiaxial loading, no such consensus has been reached, yet. Many of the recently developed models concentrate on transient effects like out-of-phase hardening, cyclic hardening or softening, and ratchetting or relaxation. For uniaxial loading most of these models cannot even be reduced to the 'MASING plus memory' model. Almost all of these models have very limited memory properties not capable of simulating multiply inserted hystereses under variable amplitude loading and most of them predict quite different mean stresses under constant amplitude loading with non-zero mean strain.

As already stated, the models for notch analysis proposed in this paper set up a general framework, which can be used with most multiaxial deformation models including those aimed at modelling transient effects. For the examples and a less abstract derivation of the proposed notch analysis approach, the MRÓZ model [8] was selected as reference material model. MRÓZ type models are the only ones which can be reduced to the 'MASING

plus memory' model in uniaxial loading, simplifying comparison of the new approach with older ones for notch analysis under uniaxial or proportional loading. Three variants of the MRÓZ model have been published: the original discrete yield surface model [8], the continuous yield surface model by CHU [9], and the continuous yield surface model using an integral flow rule by BROKATE, DRESSLER and KREJČÍ [10]. The three models predict very different behaviour for 'unbalanced' loading paths leading to ratchetting or mean stress relaxation: the original model shows rather large discretisation effects [11], but converges to the model of CHU for a large number of yield surfaces. Both models predict a constant ratchetting rate for 'unbalanced' multiaxial loading paths, and no ratchetting for uniaxial loading. The model of BROKATE *et al.* predicts stable response under any type of loading, and can be analytically inverted between stress and strain control. It seems to be the best generalization of the uniaxial 'MASING plus memory' model to multiaxial loading. Still, the original model was used in the context of this paper for two reasons: First of all, it is well known and an implementation of the model into the finite element code of ABAQUS is publically available as source code [12]. This code was also used as basis of the notch analysis code. Secondly, the extremely large amount of ratchetting or mean stress relaxation predicted by this model emphasizes the effects of stress or strain control at the notch root. From this point of view the original MRÓZ model was considered more difficult for the proposed notch analysis approach than many other material models.

It may be seen as overly ambitious to attempt to model notch root response at all, given the current state of the art of material modelling. However, the framework developed here can include better models, when they become available, even if certain effects like ratchetting are grossly overestimated by the currently used reference model.

4 A MODEL FOR NOTCH RESPONSE UNDER CYCLIC LOADING

Three different types of 'multiaxiality' determine notch analysis: External loading, i.e. the number of independently acting load components, stress state at the point of the structure to be analyzed, and stress states in the rest of the structure.

4.1 Uniaxial stress state at the notch root

In 'uniaxial' notch analysis, *notch* response under cyclic loading has been modelled just like the *material*'s response. Assuming the deformation behaviour of the material can be modelled using MASING's hypothesis and appropriate memory rules, a *structural* 'MASING plus memory' model is defined by applying those same rules to the load-notch strain curve instead of the uniaxial stress-strain curve.

Formally written, this means that when the cyclic deformation behaviour of the material is defined by the cyclic stress-strain curve

$$\varepsilon = g(\ \sigma\ ), \tag{13}$$

MASING behaviour [5] of all hysteresis branches

$$\Delta\varepsilon \cdot \mathrm{sgn}(\Delta\sigma) = 2 \cdot g(\ |\Delta\sigma|/2\ ), \tag{14}$$

and memory rules [6, 7] defined for σ, then the corresponding structural 'MASING plus memory' model is defined by the cyclic load-notch strain curve

$$\varepsilon = f(\ {}^{e}\sigma\ ), \tag{15}$$

MASING behaviour of all load-notch strain hysteresis branches

$$\Delta\varepsilon \cdot \mathrm{sgn}(\Delta^{e}\sigma) = 2 \cdot f(\ |\Delta^{e}\sigma|/2\ ), \tag{16}$$

and memory rules defined for ${}^{e}\sigma$. In other words, the real stress σ is replaced by the pseudo stress ${}^{e}\sigma$, but the model remains unchanged otherwise.

To the authors' knowledge this still is the only model describing *stabilized cyclic* deformation behaviour of uniaxially stressed notch roots under uniaxial loading, although a large number of suggestions for improvement exist in the closely related field of estimating the elastic-plastic load-notch strain curve for monotonic loading, Eq. (15). This approach is very effective not just for the few completely uniaxially stressed structures like beams under bending, but also for plates with holes and similar structures. Although it the existence of multiaxial stress states in the rest of the structure, it is sufficiently accurate at the load levels commonly analyzed in fatigue.

Because multiaxial stress states in the rest of structure do not seem be very important for notch analysis in 'uniaxial' loading, the same should be true for multiaxial non-proportional *external loading* if the notch root is still uniaxially stressed. The uniaxial local stress at the notch root ${}^{e}\sigma$ can computed by theory of elasticity from Eq.(2). Only here is the multiaxial loading introduced into the analysis. The model defined by Eqs. (15) and (16) remains unchanged. This approach has been used by SEEGER *et al.* in [13, 14, 15] for plates with holes. They checked it for cyclic loading by finite element analyses using the deformation model of PRAGER-ZIEGLER and sufficient accuracy at load levels typical for fatigue was obtained in these cases.

4.2 Multiaxial stress state at the notch root

It seems natural to extend this approach one large step further and cover multiaxial stress states at the notch root as well. First, a model for the cyclic deformation behaviour of the *material* under multiaxial non-proportional loading has to be selected. As already explained, the discrete model of

MRÓZ [8] (with a large number of yield surfaces) will be used as a reference, but other models could have been used.

This model has often been described and even an analytical solution for certain stress-controlled paths was obtained [11]. Just the most important elements of this model will be repeated here. The only input needed is the cyclic equivalent stress σ_q vs. equivalent plastic strain $\varepsilon_{p,q}$ curve

$$\varepsilon_{p,q} = g(\ \sigma_q\ ). \tag{17}$$

Equivalent stresses are determined by the isotropic yield criterion of VON MISES. During plastic straining a discrete or continuous set of yield surfaces, defined by the VON MISES criterion and originally concentric to the origin, moves in stress space following MRÓZ' kinematic hardening rules. Total strains are decomposed into their elastic and plastic parts by

$$\mathrm{d}\epsilon = \mathrm{d}\epsilon^e + \mathrm{d}\epsilon^p \tag{18}$$

and plastic strain increments are determined by the normality flow rule.

Again, the model for deformation of the *material* is stated for the *structural* behaviour by replacing the real stress tensor σ_{ij} with the pseudo stress tensor ${}^e\sigma_{ij}$.

The only additional consideration necessary deals with the nature of plastic strains in Eq. (17). From the uniaxial cyclic stress vs. total strain curve, plastic strains are easily computed as

$$\varepsilon_{p,q} = \varepsilon_{t,q} - \sigma_q/E. \tag{19}$$

If, however, the cyclic load-notch strain curve is defined in terms of real plastic equivalent strain at the notch root vs. equivalent pseudo stress

$$\varepsilon_{p,q} = f(\ {}^e\sigma_q\ ) \tag{20}$$

the following inequality holds after yielding

$$\varepsilon_{p,q} \neq \varepsilon_{t,q} - {}^{e}\sigma_q/E \tag{21}$$

as shown in Fig. 2. If the latter approach is used, the plastic notch strains computed by the *structural* model for a given ${}^{e}\sigma_{ij}(t)$ time history must then be fed into the *material* model to compute real notch stresses and real total notch strains. This approach is identical to the approach of BARKEY *et al.*, if the differences in yield criteria are accounted for.

Obviously one alternative to this stress based approach is a strain based one, i.e. defining the basic structural stress-strain curve as (real) equivalent notch stress σ_q vs. pseudo notch strain based on theory of elasticity ${}^{e}\varepsilon_q$

$$\sigma_q = \mathcal{F}({}^{e}\varepsilon_q), \tag{22}$$

thus using pseudo strains to compute local elastic-plastic stresses with the *structural* model and then calculating real notch-strains from them using the *material* model. Because pseudo stresses and strains are related through the elasticity tensor of the material

$${}^{e}\varepsilon_{kl} = E^{(-1)}_{ijkl} \cdot {}^{e}\sigma_{ij} \tag{23}$$

this alternative yields identical results for stable material behaviour and uniaxial loading. For transient material behaviour and/or multiaxial loading, however, quite different results are obtained similar to stress or strain controlled tests of unnotched specimens.

4.3 ${}^{e}\sigma$ based approach

Thus, the ${}^{e}\sigma$ based multiaxial notch analysis proposed here consists of the following steps:

1. Determine the proportionality constants $c_{ij,m}$ via separate structural analyses based on theory of elasticity for each unit load $|L_m| = 1$.

2. Determine a basic ${}^e\sigma_q$-$\varepsilon_{p,q}$ curve for monotonic loading using elastic-plastic finite element analysis, strain measurements or a suitable uni-axial approximation formula.

3. Compute the history of the local fictitious stress tensor ${}^e\sigma_{ij}(t)$ from Eq. (2).

4. Apply this history to a *stress-controlled* deformation model (here: the Mróz model) using the VON MISES yield criterion and the basic ${}^e\sigma_q$-$\varepsilon_{p,q}$ curve of step 2, thereby computing the (real) local *plastic* strain history.

5. Take this plastic strain history to compute deviatoric stresses using the normality rule and then 'real' stresses and elastic strains using the same deformation model as in step 4. In general at least one stress component has to be known in advance in order to determine the missing hydrostatic pressure. For MRÓZ type models and most two surface models this step can be both simplified and generalized as is shown in the appendix.

Steps 3 to 5 do not have to be sequential for the whole history, only for each time step. Depending on the local boundary conditions at the notch root, suitable sub-spaces like plane stress or plane strain have to be used in the deformation models of steps 4 and 5. Also, pressure acting on the notch surface can be considered. An advantage of using ${}^e\sigma$ as the governing variable is that the same boundary conditions apply to ${}^e\sigma_{ij}$ as to σ_{ij}, which would not be case for nominal stresses S.

4.4 $^e\varepsilon$ based approach

Similarly, the $^e\varepsilon$ based notch analysis consists of the following steps:

1. Determine the proportionality constants $c_{ij,m}$ as in the $^e\sigma$ based approach.
2. Determine a basic σ_q-$^e\varepsilon_q$ curve for monotonic loading.
3. Compute the history of the local pseudo strain tensor $^e\varepsilon_{ij}(t)$ from Eqs. (2) and (23).
4. Apply this history to a *total strain-controlled* deformation model (here: the Mróz model) using the VON MISES yield criterion and the basic σ_q-$^e\varepsilon_q$ curve of step 2, thereby computing the (real) local stress history.
5. Take this stress history to compute (real) elastic-plastic total strains from a stress-controlled version of the same deformation model as in step 4, but using the *material's* σ-ε curve as the basic stress strain curve.

5 PROPORTIONAL LOADING

The ability to model proportional or non-proportional loading and uniaxial or multiaxial notch stress-states in a unified way seems to be a major—theoretical—strength of this approach. However, as for any estimation procedure, only a quantitative comparison between real and predicted behaviour can be used to decide about the suitability of the procedure. Few data is available for non-proportional loading. For proportional loading, however, test data [16, 17] and finite element results have been published [18, 19, 20]. Also a number of notch strain approximation procedures for proportional

loading have been proposed [18, 21, 22]. Some interesting features may be discussed by first looking at proportional loading and comparing with the approximation procedure of HOFFMANN and SEEGER.

5.1 Plane stress

For proportional loading and a local plane stress state as shown in Fig. 1 it is possible to solve the proposed procedure analytically. In this case the local pseudo stresses based on theory of elasticity depend linearly on just one external 'load'

$$ {}^{e}\sigma_z = c_z \cdot L, \quad {}^{e}\sigma_x = c_x \cdot L, \quad {}^{e}\tau_{xz} = c_{xz} \cdot L, \tag{24} $$

thus the ratio of the corresponding deviatoric stress components remains constant throughout the loading. Therefore the ratio of the plastic strain components must also remain constant and the integration of the PRANDTL-REUSS equations then leads to HENCKY's flow rule (deformation theory of plasticity). This means that external proportional loading is modelled as 'radial loading' in terms of ${}^{e}\sigma_{ij}$. The ratio of the plastic strain components may now be computed from the normality rule, i.e. the ratio of plastic strain components is same as the ratio of the components of the local 'elastic' deviatoric stress tensor ${}^{e}s_{ij}$.

For a state of plane stress at the considered structural location the plastic strain components are

$$ \varepsilon_{p,z} = \frac{c_z - 0.5\, c_x}{c_q}\, \varepsilon_{p,q} \tag{25} $$

$$ \varepsilon_{p,x} = \frac{c_x - 0.5\, c_z}{c_q}\, \varepsilon_{p,q} \tag{26} $$

$$ \varepsilon_{p,y} = -0.5\, \frac{c_z + c_x}{c_q}\, \varepsilon_{p,q} \tag{27} $$

$$ \gamma_{p,xz} = 3\, \frac{c_{xz}}{c_q}\, \varepsilon_{p,q} \tag{28} $$

where c_q is the proportionality constant corresponding to the VON MISES stress

$$c_q = \sqrt{c_x^2 + c_z^2 - c_x\ c_z + 3\ c_{xz}^2}. \tag{29}$$

The equivalent plastic strain may be computed using the equivalent load-total notch strain curve

$$\varepsilon_{t,q} = f({}^e\sigma_q) = f(c_q \cdot L) \tag{30}$$

and the equivalent stress-total strain curve of the material

$$\varepsilon_{t,q} = g(\sigma_q), \qquad \sigma_q - g^{-1}(\varepsilon_{t,q}) \tag{31}$$

as

$$\varepsilon_{p,q} = \varepsilon_{t,q} - \sigma_q/E. \tag{32}$$

Note that in Eq. (32) the 'real' stress σ and not the pseudo stress ${}^e\sigma$ is used.

With the known local plastic strains the local deviatoric stress tensor s_{ij} can be computed from HENCKY's rule

$$s_{ij} = \frac{2}{3}\ \frac{\varepsilon_{p,ij}}{\varepsilon_{p,q}}\ \sigma_q \tag{33}$$

For a general stress state Eq. (33) is not sufficient to compute the local stress tensor. For plane stress, however, the stress normal to the surface must be zero. The missing hydrostatic pressure $\bar{\sigma}$ can therefore be computed from

$$\sigma_y = s_y + \bar{\sigma} = 0. \tag{34}$$

Thus the local stresses are simply

$$\sigma_z = \frac{c_z}{c_q}\sigma_q \tag{35}$$

$$\sigma_x = \frac{c_x}{c_q}\sigma_q \tag{36}$$

$$\tau_{xz} = \frac{c_{xz}}{c_q}\sigma_q. \tag{37}$$

The elastic strains are then given by

$$\varepsilon_{e,z} = \frac{c_z - \nu\, c_x}{c_q}\, \varepsilon_{e,q} \tag{38}$$

$$\varepsilon_{e,x} = \frac{c_x - \nu\, c_z}{c_q}\, \varepsilon_{e,q} \tag{39}$$

$$\varepsilon_{e,y} = -\nu\, \frac{c_z + c_x}{c_q}\, \varepsilon_{e,q} \tag{40}$$

$$\gamma_{e,xz} = 2(1+\nu)\, \frac{c_{xz}}{c_q}\, \varepsilon_{e,q} \tag{41}$$

with $\varepsilon_{e,q} = \sigma_q / E$.

A constant ratio of plastic strain and of deviatoric stress tensor components is predicted. For plane stress the ratio of the stress and elastic strain components is constant, too. For pressure loading on the notch surface, however, this would not be the case.

The ratio of the total strain components depends on $\varepsilon_{e,q}/\varepsilon_{p,q}$. Only for the trivial case of a linear equivalent load-notch strain curve a constant ratio of the total strain components is predicted.

5.2 The approach by HOFFMANN and SEEGER

The load-notch strain approximation for proportional loading by HOFFMANN and SEEGER [18, 23, 24] also builds on a load-notch strain curve defined for equivalent quantities like Eq. (30). Validity of deformation theory is assumed, therefore HENCKY's equations can be written as a generalized form of HOOKE's law for plane stress

$$\varepsilon_{t,z} = \frac{\varepsilon_{t,q}}{\sigma_q} \left(\sigma_z - \nu'\, \sigma_x\right) \tag{42}$$

$$\varepsilon_{t,x} = \frac{\varepsilon_{t,q}}{\sigma_q} \left(\sigma_x - \nu'\, \sigma_z\right) \tag{43}$$

$$\varepsilon_{t,y} = -\frac{\varepsilon_{t,q}}{\sigma_q}\, \nu' \left(\sigma_z + \sigma_x\right) \tag{44}$$

$$\gamma_{t,xy} = \frac{\varepsilon_{t,q}}{\sigma_q} 2(1+\nu')\,\tau_{xz} \tag{45}$$

with

$$\nu' = 0.5 - (0.5-\nu)\frac{\sigma_q}{E\ \varepsilon_{t,q}}. \tag{46}$$

This approach allows the specification of exact mechanical 'boundary conditions' at the examined location, if these exist, or an additional assumption. The default assumption is that the ratio of principal total strains remains constant throughout the loading. However, other assumptions are possible, e.g. a constant ratio of stress components. In this case individual stress components may be written as

$$\sigma_z = \frac{c_z}{c_q}\sigma_q, \quad \sigma_x = \frac{c_x}{c_q}\sigma_q, \quad \tau_{xz} = \frac{c_{xz}}{c_q}\sigma_q. \tag{47}$$

With

$$\varepsilon_{t,q} = \varepsilon_{e,q} + \varepsilon_{p,q} \tag{48}$$

$$\sigma_q = E \cdot \varepsilon_{e,q} \tag{49}$$

Eqs. (42) – (45) for the total strains can then be written as

$$\varepsilon_{t,z} = \frac{c_z - \nu\ c_x}{c_q}\ \varepsilon_{e,q} + \frac{c_z - 0.5\ c_x}{c_q}\ \varepsilon_{p,q} \tag{50}$$

$$\varepsilon_{t,x} = \frac{c_x - \nu\ c_z}{c_q}\ \varepsilon_{e,q} + \frac{c_x - 0.5\ c_z}{c_q}\ \varepsilon_{p,q} \tag{51}$$

$$\varepsilon_{t,y} = -\nu\ \frac{c_z + c_x}{c_q}\ \varepsilon_{e,q} - 0.5\ \frac{c_z + c_x}{c_q}\ \varepsilon_{p,q} \tag{52}$$

$$\gamma_{t,xz} = 2(1+\nu)\frac{c_{xz}}{c_q}\ \varepsilon_{e,q} + 3\ \frac{c_{xz}}{c_q}\ \varepsilon_{p,q} \tag{53}$$

which shows that for proportional loading and a local state of plane stress the ${}^{e}\sigma$ based approach proposed here delivers the same results as the approach of HOFFMANN and SEEGER for the—non-default—assumption of a constant stress ratio.

5.3 Special cases of plane stress

Analyzing the notch response predicted by the ${}^{e}\sigma$ based approach proposed here, for a local plane stress state with either decreasing or increasing notch constraint the following behaviour is found:

- For *decreasing* notch constraint the exact solution is obtained in the limit case of a smooth bar.
- For *increasing* notch constraint, typical for deep and sharp notches in round bars, the solution should approach a state of plane strain locally ($\varepsilon_x = 0$, $c_x = \nu\ c_z$). From Eq. (51) it can be seen that this would require

$$(1 - 0.5/\nu) \cdot \varepsilon_{p,q} = 0, \tag{54}$$

  a condition violated with increasing amount of plasticity.

The load-notch strain approximation approach of HOFFMANN and SEEGER, on the other hand, assumes—in the default case—a constant ratio of total strain components, forced upon the notch by the surrounding elastic material. It is therefore not exact for the limit case of a smooth bar, but for severely constrained bars. As already shown in the previous subsection the default assumption of a constant principal total strain ratio can be changed, however, to either match exact mechanical 'boundary conditions' at the examined location or to use more appropriate assumptions such as a constant ratio of stress components for bars with diminishing notch constraint.

5.4 Comparison with finite element analyses

Finite element analyses were conducted for a mild and a sharp notched round bar. Five combinations of axial (S_Z) and torsional (S_{XZ}) loads were

analysed and three cyclic stress-strain curves were used. Tab. 1 contains the geometry, loading, and materials data. The analyses were done using ABAQUS.

There are three separate sources for errors in both load-notch strain approximation schemes:

1. inaccuracies of the equivalent load-notch strain curve,
2. errors induced by the change of the structural behaviour above net section yield, and
3. errors accompanying the decomposition of the equivalent quantities at lower load levels.

Certainly the errors induced by using one of the common uniaxial load-notch strain approximation formulas can be rather large. But this is well known, and it could be cured by performing a *single* elastic-plastic finite element analysis for any ratio S_Z/S_{XZ}. After all, the new approach predicts that all curves of equivalent pseudo stress ${}^e\sigma_q$ vs. equivalent notch strain ε_q should be the same—regardless of the load ratio S_Z/S_{XZ}. Fig. 3 shows the results of the finite analyses in this regard. Clearly, the curves are significantly different at high load levels. Of course this was expected, because a simple calculation already shows the fully plastic limit loads to be quite different even for unnotched bars under axial or torsional loading. In the examples shown here the constraint introduced by the notch increases the limit load for axial loading very drastically. Still, at low and intermediate load levels the equivalent load-notch strain curve from a *single* finite element analysis would be a better approximation for a different load case than using an approximation formula.

It should be noted here, that HOFFMANN and SEEGER actually designed

their approach to use the generalization of [1], i.e. to determine different equivalent load-notch strain curves for different load ratios. However, knowledge of the fully plastic limit load is needed then, which often requires additional finite element analyses.

In a second step the ability to decompose the equivalent load-notch strain curve into individual stress and strain components is tested for the three different approaches—the $^{e}\sigma$ based approach (identical to constant stress ratio HOFFMANN and SEEGER as already shown analytically), the $^{e}\varepsilon$ based, and the constant strain ratio HOFFMANN and SEEGER approach. In order to separate both errors, the local stress-strain curves shown in Fig. 4 and 5 for the three approximations are based on the *individual* equivalent load-notch strain curve *as determined by finite element analysis* and shown in Fig. 3. Thus a given load level corresponds to the same total and plastic strains in the finite element analyses and in the approximations. The points corresponding to equivalent plastic strains $\varepsilon_{p,q} = 0.1,\ 0.2,\ 0.5,\ 1.0\%$ were marked with dots and crosses, enabling a comparison at different load levels.

For the sharp notch and the stiff material, Fig. 4, the axial (σ_z-ε_z) and torsional (τ-γ) stress-strain curves of the finite element analyses were approximated rather well by all approaches. Only the constant strain ratio approach, however, allowed a good estimation of the circumferential strains (σ_x-ε_x). The $^{e}\sigma$ approach drastically underestimates the notch constraint during plastic straining in this case, and therefore predicts too large strains and too small stresses. It should be noted that the circumferential strains remain much smaller than the axial and torsional strains, and therefore have less significance for fatigue life prediction. Results between these two extremes were obtained for the $^{e}\varepsilon$ approach, which actually implements mixed strain and stress control—primarily strain control, but subsequently stress control, too. Neither the real stress ratio, nor the real strain ratio is constant in this case. For pure torsional loading the decomposition of the equivalent

stress-strain curve is exact for all approximation methods, which is trivial.

Results for the mild notch and the medium material are depicted in Fig. 5. Looking at pure axial loading first, the finite element analyses show the expected results of a decreasing notch constraint at higher load levels. They start off at the curves of the constant strain ratio approximation, move towards the curves of the constant strain ratio approximation at intermediate levels, and even intersect these at higher load levels, i.e. for fully plastic specimens. Due to the shear stress gradient induced by torsion the axial stresses increase in the interior of the net-section, where the shear stresses are small, and decrease near the notch, where the shear stresses are high, to fulfill the equivalent stress-strain curve. Fig. 5 clearly shows that the ${}^{e}\sigma$ approximation is *not* the limit case for mildly notched components. The redistribution of stresses and strains in the net section accompanying fully plastic states leads to non-monotonic component stress-strain curves – in spite of a corresponding monotonically increasing equivalent load-notch strain curve, Fig. 3. A particular drastic example for this is the load combination $S_Z/S_{XZ} = \sqrt{3}/2$, where even for the sharp notch and the stiff material a similar behaviour can be found in Fig. 4. Again, the results for the ${}^{e}\varepsilon$ approximation lie between the extremes of constant strain or constant stress ratio, respectively.

The results found in this study of proportionally loaded, notched round bars can be generalized as follows:

1. Stress-strain response of sharply notched components is most accurately approximated by the constant strain ratio approach, but the errors of the ${}^{e}\sigma$ approach only affect the circumferential stress and strain, i.e. the smallest and least significant components of the stress and strain tensors.

2. For mildly notched specimens the ${}^{e}\sigma$ approximation is sufficiently ac-

curate in the—very small—range between onset of yielding and fully plastic state.

3. The ${}^{e}\varepsilon$ approximation predicts results between the extremes of the constant strain ratio and the ${}^{e}\sigma$ approach.

4. The constant stress or strain ratio approximations do *not* describe *limits* of actual notch response, due to the significant changes of structural behaviour in the fully plastic state, which for mildly notched specimens may correspond to rather low local strains.

5. Non-monotonic local stress-strain response can be found even for these 'standard' specimens, just like it was found for pressurized components before [20].

6. All approximation approaches predict local strains more accurately than local stresses (compare the dot and cross symbols in Figs. 4 and Fig. 5).

6 NON-PROPORTIONAL LOADING

To demonstrate the performance of the proposed models for non-proportional loading, comparisons with results of finite element analyses will be shown for two 'balanced' loading paths and one 'unbalanced' loading path leading to mean stress relaxation. Again, the finite element analyses were done with ABAQUS using an implementation of the MRÓZ model [12].

Also, all results of the approximations are based on equivalent load-notch strain curves (${}^{e}\sigma_q$ vs. $\varepsilon_{p,q}$, and σ_q vs. ${}^{e}\varepsilon_q$, respectively) determined by monotonic elastic-plastic finite element analyses. Averaging the differences between the equivalent load-notch strain curves for different load ratios S_Z/S_{XZ} as shown in Fig. 3, only curves for a load ratio of $S_Z/S_{XZ} = \sqrt{3}/1$

were used as input for all examples. Because the discrete yield surface MRÓZ model was used, the load-notch strain 'curves' were read as discrete points from the results files of monotonic finite element analyses. No smoothing was done. Due to the nature of h-method elastic-plastic finite element analysis the largest relative error for stresses and plastic strains at *nodes* occurs immediately after the onset of yielding, when the notch element is still only partly plastic. This explains a certain 'jaggedness', which can be seen not only in the finite element results, but also in the approximations, after an elastic segment.

6.1 Balanced load paths

Results for box and diamond loading paths using the anisotropic yield surface approach of BARKEY *et al.* have been published elsewhere [2, 3, 4]. Results obtained with the ${}^{e}\sigma$ and the ${}^{e}\varepsilon$ based approximations for these paths are very close to the published results, and thus omitted here.

The first example presented in Fig. 6 is for a 'X' path, in which linear segments between zero and maximum are cycled counter-clockwise. The basic 'X' path was repeated ten times. The results shown were obtained for the mild notched round bar and the stiff material described in Tab. 1. As explained in the appendix, the real stress increments predicted by the ${}^{e}\sigma$ approach are just scaled down from the applied pseudo stress increments. Here this leads to a σ vs. τ phase diagram very similar to the original load path. The non-linear interaction between shear stress and axial stress found in the finite element results and the ${}^{e}\varepsilon$ approximation is missing in the ${}^{e}\sigma$ approximation. The total strain amplitudes predicted by both approximations are very good, however the stress amplitudes and the interaction between shear and normal strain are modelled better by the ${}^{e}\varepsilon$ approximation.

In the second example, depicted in Fig. 7, sinusoidal loading with dif-

ferent frequencies in axial and torsional directions was used. Five cycles of the torsional loading were applied during one cycle of the axial loading. The results shown are for four cycles of the axial loading, after which the notch response was stable. Again, the stiff material was used, but the structure analysed was the sharp notched round bar. Very good predictions were obtained for the ${}^{e}\varepsilon$ approach — slightly better for the local stresses than for the local strains. This can generally be expected, because in the ${}^{e}\varepsilon$ approach stresses are computed first, and strains only afterwards. Thus, predicted strains are more susceptible to errors than stresses, particularly at high load levels and for soft materials. At first look, the ${}^{e}\sigma$ approximation does not display the right characteristics, especially in the σ vs. τ phase diagram. The error in the amplitudes is not very large, but the interaction between shear and axial components is more realistically modelled by the ${}^{e}\varepsilon$ approach. The strain based approach may seem to be especially well suited to the sharp notch of this example, due to the higher circumferential notch constraint, but similar results were found for the mild notch loaded with the same path.

6.2 Unbalanced load paths

A particularly difficult problem for non-proportional deformation modelling is multiaxial ratchetting, i.e. the accumulation of plastic strain due to certain types of multiaxial stress controlled loading paths, and the inverse effect of mean stress relaxation due to multiaxial loading. We will refer to loading paths causing either phenomenon as 'unbalanced paths'. Most multiaxial deformation models predict ratchetting or mean stress relaxation for such multiaxial paths, especially those two- or multi-surface models based on MRÓZ' kinematic hardening rules. Often the predicted ratchetting or relaxation rate is too high in comparison to experimental data. It has been shown that a MRÓZ model with an infinite number of yield surfaces either

predicts a *constant ratchetting rate* [11] for unbalanced loading paths or *no ratchetting* at all, e.g. for uniaxial loading.

Fig. 8 depicts results for the sharp notch and the stiff material loaded with constant torsion and cyclic axial force. Only the first 10 cycles are shown. A mixture of relaxation of the shear mean stress and accumulation of the plastic shear strain is predicted by the finite element analysis, again using the MRÓZ model with a large number of yield surfaces. During the first few cycles the shear stress is reduced significantly, thereby reducing the rate of plastic strain accumulation, too. However, because the shear stress is not yet zero, and because the cyclic axial loading itself is in the plastic range, a small rate of plastic shear strain accumulation is predicted even for the next cycles. Similar results have been obtained for the mild notch and for other materials, as long as the net section of the notched bar remained partly elastic. With increasing amount of plasticity the rate of stress relaxation is reduced and strain accumulation is increased. At load levels much higher than shown in Fig. 8, i.e. when the net section was already fully plastic, a linear accumulation of plastic shear strains was computed in the finite element analysis.

The ${}^{e}\sigma$ and the ${}^{e}\varepsilon$ based approximations predict very different results for such unbalanced paths. The ${}^{e}\sigma$ based approximation has to predict a linear accumulation of shear strains regardless of the amount of net section plasticity, because this is the nature of a MRÓZ model for similar stress-controlled paths. As shown in the appendix, the ${}^{e}\sigma$ approximation—though formally using mixed stress/strain control—is in fact purely stress controlled, because increments of pseudo stress ${}^{e}\sigma$ and real stress σ always have the same direction. The ${}^{e}\varepsilon$ based approximation first computes real notch stress response in a strain controlled mode, and then real notch strains in a stress controlled mode. This mixed control nicely reflects the finite element results: mean shear stress relaxation leading to decreased shear strain accumulation

rates.

Thus, the τ vs. γ notch response during the first cycles is predicted quite well by the ${}^{e}\varepsilon$ based approximation, whereas the small, but non-zero, strain accumulation during later cycles predicted by the finite element analysis was not approximated correctly by ${}^{e}\varepsilon$. This effect is essentially non-local, i.e. related to a stress redistribution in the net-section. The ${}^{e}\sigma$ based approximation predicts a constant ratchetting rate and no shear stress relaxation, which is inconsistent with the finite element results. The axial strains are approximated accurately in both cases. Similar effects would be found in proportional loading if a deformation model accounting for uniaxial ratchetting were used.

Most components with sharper notches will not exhibit a significant amount of ratchetting under typical fatigue loading. The ${}^{e}\varepsilon$ approximation is best suited for these cases, whereas the ${}^{e}\sigma$ approach might be used at high load levels for components with mild notches.

7 ADVANTAGES

A model based on local stresses computed by theory of elasticity ${}^{e}\sigma_{ij}$ has been proposed which is a natural extension of earlier approaches to use a given *material* model for describing *structural* notch root deformation.

1. The same model can be used for uniaxial or multiaxial loading and stress states, i.e. all structural limit cases are included.

2. The use of local stresses based on theory of elasticity instead of nominal stresses makes it easy to use this approach as part of the postprocessing of finite element analyses.

3. Unlike the procedure suggested in [24] for multiaxial stress states, the approach proposed here is not iterative. Its computational expense is equivalent to performing two cyclic analyses of the same number of cycles with a *material* model. This can be done on low-end computers.

4. It is not necessary to implement HILL's yield criterion in the deformation model. Any readily available deformation model using the VON MISES yield criterion can be used to compute the local plastic strains. For the ${}^{e}\sigma$ based approach a slight modification of standard implementations is necessary to compute local stresses from given *plastic* strains. The ${}^{e}\varepsilon$ approach consists of a straight-forward combination of standard implementations.

5. The suggested formulation describes the onset of yielding for any structure and any number of loads invariant of the coordinate system and type of loading.

6. Only a *local* coordinate system is used, easing the derivation of solutions for some local boundary conditions such as pressure on the notch surface.

7. Materials obeying different yield criteria (e.g. the TRESCA criterion) may be analyzed immediately with the proposed re-formulation. For the approach by BARKEY *et al.*, however, an *anisotropic* TRESCA criterion would have to be derived and implemented first.

8 FURTHER REFINEMENT

The results known so far suggest two areas for improvement

1. Clearly, the single equivalent load-notch strain approach is not valid at high load levels. Also ratchetting or stress relaxation at the notch

depend very much on the stress level in the net section. It may be possible to extend the approach proposed here in a similar manner as in [1] for uniaxial stress states, by modelling fully plastic net section behaviour with an additional anisotropic yield surface.

2. No equivalent to the constant principal total strain ratio approach of HOFFMANN and SEEGER, which so successfully models proportional loading of sharply notch components, has yet been derived. Such an approach might be valuable for sharp notches with high local constraint, but it would have to use two different deformation models — one for modeling the structural behaviour, and a different model for the material behaviour. This would allow use of different flow rules for structural and material behaviour, which is essentially what HOFFMANN and SEEGER proposed. The different deformation models might, however, lead to inconsistencies, e.g. in the local boundary conditions. Further research in this direction is necessary.

ACKNOWLEDGEMENTS

The authors would like to thank Prof. T. Seeger and Dr. H. Amstutz of Technische Hochschule Darmstadt (FRG) for many discussions concerning load-notch strain approximations, and especially Dr. M. Hoffmann of Mechanical Dynamics GmbH, Marburg (FRG), for his helpful suggestions.

APPENDIX: CALCULATION OF REAL STRESSES IN THE ${}^{e}\sigma$ APPROACH

In the following a shortcut to calculate real stresses and strains for the ${}^{e}\sigma$ approach in one step instead of two will be derived. It also explains, why the ${}^{e}\sigma$ approach can be considered purely stress controlled — unlike the ${}^{e}\varepsilon$ approach, which implements a mixed strain and stress control.

The following derivation assumes use of the discrete yield surface MRÓZ model. It also assumes that the discretisation of the load-notch strain curve and of the material's stress-strain curve is done by selecting points with identical plastic strains for both curves. However, the results are applicable to other MRÓZ models and many two-surface models. They are only valid for stress states not including the applied load, i.e. not for notch surfaces under pressure.

In the first step of the approximation procedure, local plastic strains increments are determined by a conventional cyclic plastic approach based on the normality rule from known deviatoric pseudo stresses ${}^{e}s_{ij}$ and known pseudo backstresses ${}^{e}\alpha_{ij}$

$$\mathrm{d}\,\varepsilon_{p,ij} = \mathrm{d}\,{}^{e}\lambda\ ({}^{e}s_{ij} - {}^{e}\alpha_{ij})\,. \tag{55}$$

Subsequently, the deviatoric real stresses s_{ij} are computed from this plastic strain increment

$$\mathrm{d}\,\varepsilon_{p,ij} = \mathrm{d}\,\lambda\ (s_{ij} - \alpha_{ij})\,. \tag{56}$$

Thus, yield surface normals at the active point must be same in pseudo stress space and in real stress space. Also, the next higher yield surface must be touched at the same time in both stress spaces, because both yield surfaces correspond to the same equivalent plastic notch strain. The latter requirement can only be fulfilled if the real stresses and backstresses are just

scaled down from the pseudo stresses by a scalar, which corresponds to the ratio of distances between the active and the next higher yield surface. This ratio is identical to the ratio of the work-hardening moduli of the load-notch strain curve ${}^{e}H'$ and of the stress-strain curve H'

$$\mathrm{d}\,\alpha_{ij} = \frac{{}^{e}H'}{H'}\,\mathrm{d}\,{}^{e}\alpha_{ij} \tag{57}$$

$$\mathrm{d}\,s_{ij} = \frac{{}^{e}H'}{H'}\,\mathrm{d}\,{}^{e}s_{ij}. \tag{58}$$

In other words: for the ${}^{e}\sigma$ approach, each *increment* of the real stress tensor has the same direction as the corresponding increment of the pseudo stress tensor, but it is smaller by the ratio of the current slopes of the equivalent stress-strain curves.

REFERENCES

[1] T. Seeger, P. Heuler (1980). Generalized application of Neuber's rule. *J. of Testing and Evaluation*, 8(4), 199–204.

[2] M.E. Barkey (1993). *Calculation of Notch Strains under Multiaxial Nominal Loading.* PhD thesis, University of Illinois at Urbana-Champaign.

[3] M.E. Barkey, D.F. Socie, K.J. Hsia (1994). A Yield Surface Approach to the Estimation of Notch Strains for Proportional and Nonproportional Cyclic Loading. *J. Engng. Materials and Technology, Trans. ASME*, 116, 173–180.

[4] M.E. Barkey, D.F. Socie (1994). Calculation of Notch Strains for Nonproportional Cyclic Loading using a Structural Yield Surface. In: *Fourth International Conference on Biaxial/Multiaxial Fatigue*, Paris/France, May 31 - June 3, 1994.

[5] G. Masing (1926). Eigenspannungen und Verfestigung bei Messing. In *Proc. 2nd Int. Congress of Appl. Mechanics*, 332–335.

[6] M. Matsuishi, T. Endo (1968). Fatigue of Metals Subjected to Varying Stress. In *Proc. Kyushu Branch of Japan. Soc. of Mech. Eng.*, 37–40.

[7] U.H. Clormann, T. Seeger (1986). RAINFLOW - HCM, Ein Zählverfahren für Betriebsfestigkeitsnachweise auf werkstoffmechanischer Grundlage. *Stahlbau*, 55(3), 65–71.

[8] Z. Mróz (1967). On the Description of Anisotropic Workhardening. *J. Mech. Phys. Solids*, 15, 163–175.

[9] C.-C. Chu (1984). A Three Dimensional Model of Anistropic Hardening in Metals and its Applications to the Analysis of Sheet Metal Formability. *J. Mech. Phys. Solids*, 32, 197–212.

[10] M. Brokate, K. Dreßler, P. Krejčí (1992). A Hysteresis Operator for Rate Independent Plasticity. In: *1st World Congress of Nonlinear Analysis, Tampa, Florida.*

[11] V.B. Köttgen, T. Seeger (1993). A Masing type integration of the Mróz model for some non-proportional stress-controlled paths. *Submitted to J. Engng. Materials and Technology, Trans. ASME.*

[12] V.B. Köttgen, R.J. Anthes, T. Seeger (1991). Implementation des Werkstoffmodells von Mróz in das Finite Element Programm ABAQUS. Technical Report – Part 1: FF-7/1991, Part 2: FW-8/1991, Fachgebiet Werkstoffmechanik, Technische Hochschule Darmstadt, FRG.

[13] J. Schomburgk (1988). *Beanspruchungsermittlung und Lebensdauerabschätzung einer Lochscheibe bei zusammengesetzter Schwingbelastung.* Technical Report FS-12/1988, Fachgebiet Werkstoffmechanik, Technische Hochschule Darmstadt, FRG.

[14] P. Zacher, H. Amstutz, T. Seeger (1989). Kerbwirkungen bei zusammengesetzter Betriebsbelastung. In: H. Nowack, editor, *Kerben und Betriebsfestigkeit – 15. Vortragsveranstaltung des DVM Arbeitskreises Betriebsfestigkeit*, 329–356, DVM, Berlin, FRG.

[15] M. Hoffmann, H. Amstutz, T. Seeger (1989). Local Strain Approach in Nonproportional Loading. In: K. Kussmaul, editor, *Third International Conference on Biaxial/Multiaxial Fatigue, April 1989*, 55.1–55.20, Staatliche Materialprüfungsanstalt, Stuttgart, FRG.

[16] M. Hoffmann, T. Seeger (1985). Kerbbeanspruchungen I – Ermittlung und Beschreibung mehrachsiger Kerbbeanspruchungen im nichtlinearen Bereich. Technical Report, 115, Forschungskuratorium Maschinenbau, Frankfurt, FRG.

[17] W.N. Sharpe, K.C. Wang (1991). Evaluation of a Modified Monotonic Neuber Relation. *J. Engng. Materials and Technology, Trans. ASME*, 113, 1–8.

[18] M. Hoffmann, T. Seeger (1985). A Generalized Method for Estimating Multiaxial Elastic-Plastic Notch Stresses and Strains. Part 1: Theory. *J. Engng. Materials and Technology, Trans. ASME*, 107, 250–254.

[19] D.A. Klann, S.M. Tipton, T.S. Cordes (1993). Notch Stress and Strain Estimation Considering Multiaxial Constraint. In *SAE International Congress and Exposition*, Detroit.

[20] V.B. Köttgen, M. Schön, T. Seeger (1993). Application of a Multiaxial Load-notch Strain Approximation Procedure to Autofrettage of Pressurized Components. In: D.L. McDowell, R. Ellis, editors, *Multiaxial Fatigue*, STP 1191, 375–396, American Society for Testing and Materials, Philadelphia.

[21] N.E. Dowling, W.R. Brose, W.K. Wilson (1977). *Notched Member Fatigue Life Predictions by the Local Strain Approach*, 55–84. Volume 6 of *Advances in Engineering*, R.M. Wetzel, editor, Society of Automotive Engineers, Warrendale, PA.

[22] A. Moftakhar, G. Glinka (1992). A method of elastic-plastic stress and strain calculation at a notch root. *Submitted to J. Engng. Materials and Technology, Trans. ASME.*

[23] M. Hoffmann, T. Seeger (1985). A Generalized Method for Estimating Multiaxial Elastic-Plastic Notch Stresses and Strains. Part 2: Application and General Discussion. *J. Engng. Materials and Technology, Trans. ASME* 107, 255–260.

[24] M. Hoffmann, T. Seeger (1989). Stress-Strain Analysis and Life Predictions of a Notched Shaft Under Multiaxial Loading. In: G.E. Leese, D. Socie, editors, *Multiaxial Fatigue – Analysis and Experiments*, chapter 6, 81–101, SAE AE-14, Society of Automotive Engineers, Warrendale, PA.

List of Figures

	mild notch	sharp notch
gross section diameter D	50.8 mm	144 mm
net section diameter d	25.4 mm	120 mm
notch radius r	12.7 mm	3 mm
notch type	circle	hyperbola
$K_{t,z} = {}^{e}\sigma_z / S_Z$	1.40	2.92
$K_{t,x} = {}^{e}\sigma_x / S_Z$	0.26	0.79
$K_{t,xz} = {}^{e}\sigma_{xz} / S_{XZ}$	1.14	1.70

(Nominal stresses are defined for the net-section)

Material	E, MPa	K', MPa	n'
'soft'	210000	400	0.050
'medium'	210000	700	0.100
'stiff'	210000	1736	0.199
$\varepsilon = \sigma/E + (\sigma/K')^{1/n'}$			

loading	a	b	c	d	e
S_Z/S_{XZ}	1/0	$2\sqrt{3}/1$	$\sqrt{3}/1$	$\sqrt{3}/2$	0/1

Table 1: Geometry, loading and materials data of the finite element analyses

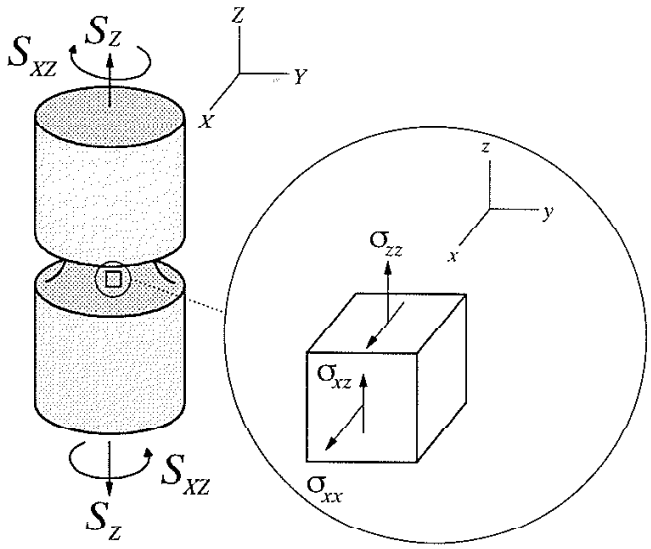

Figure 1: Notched round bar under axial and torsional loading

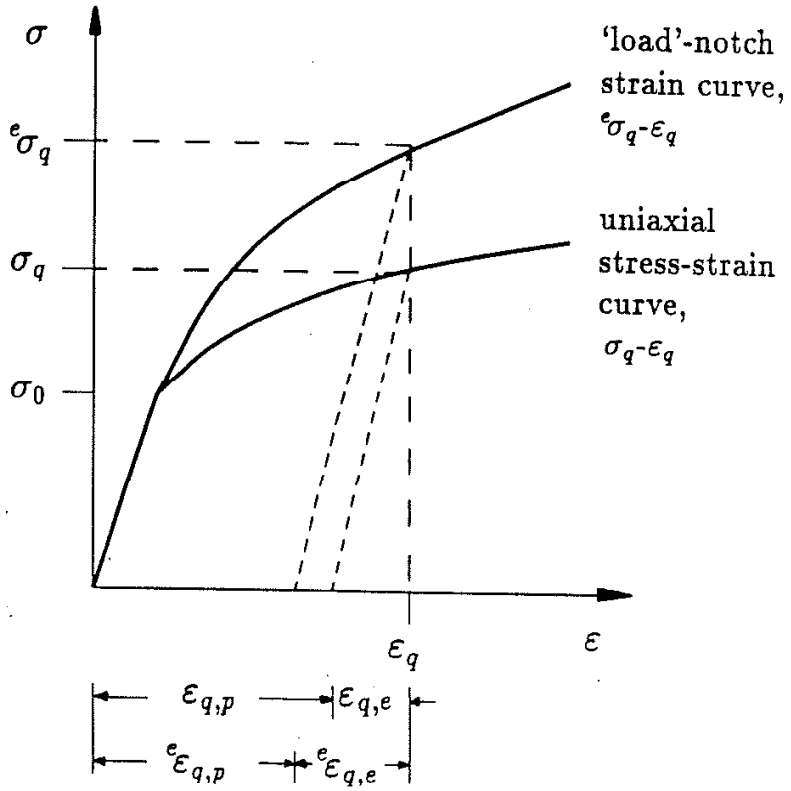

Figure 2: Decomposition of the cyclic stress-strain curve and the cyclic load-notch strain curve into elastic and plastic parts

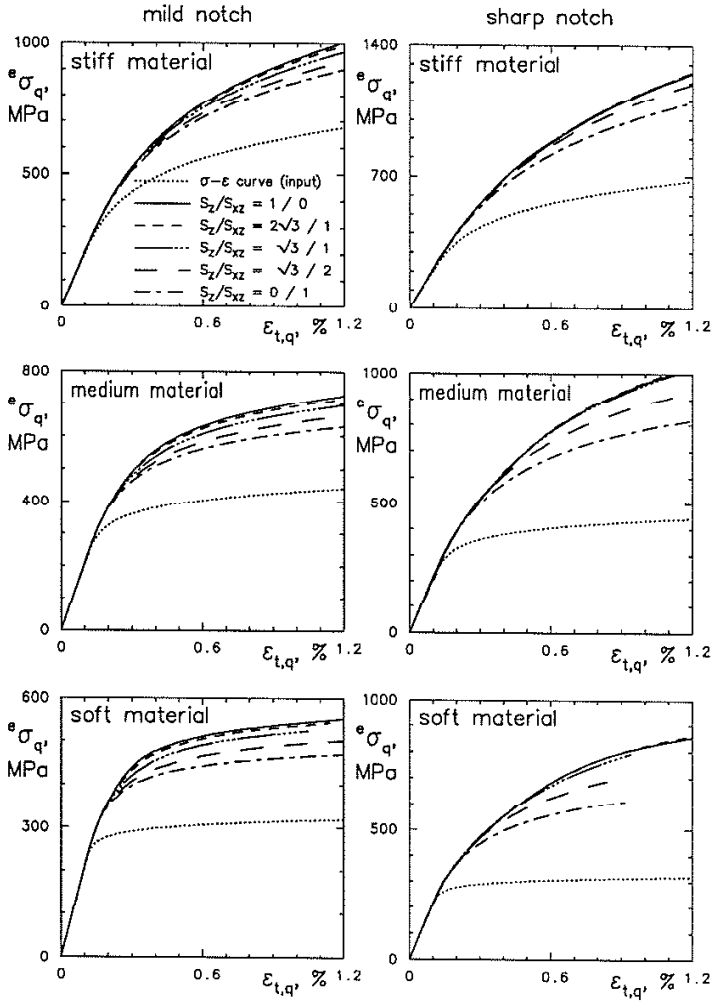

Figure 3: Equivalent load-notch strain curves for the mild and the sharp notched round bar as determined by finite element analyses

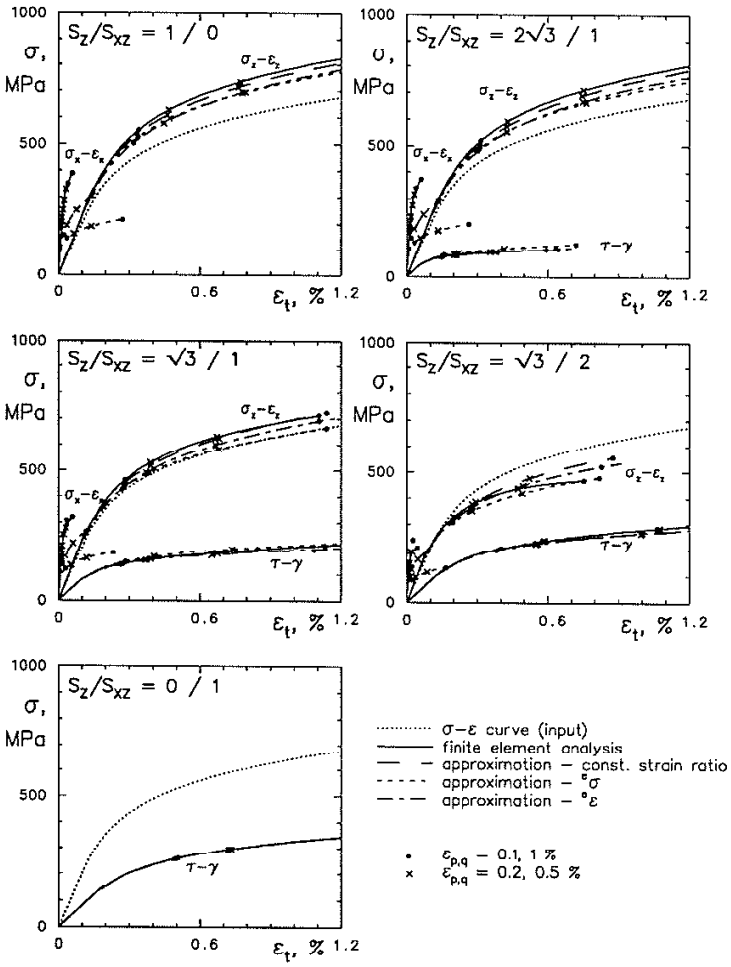

Figure 4: Local stress-strain curves for the sharp notched round bar

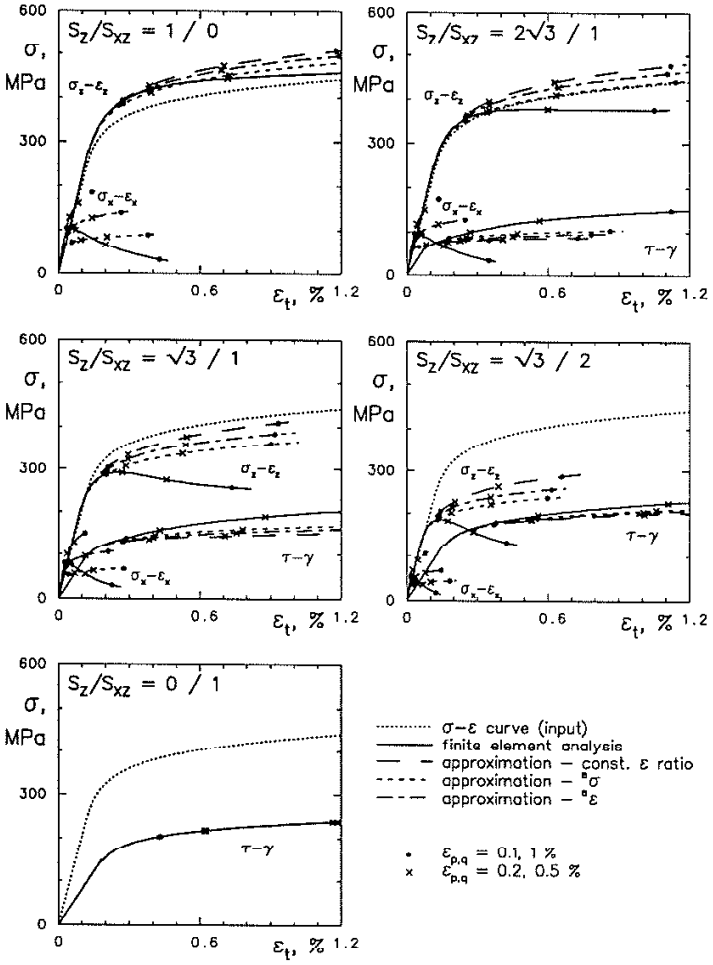

Figure 5: Local stress-strain curves for the mild notched round bar

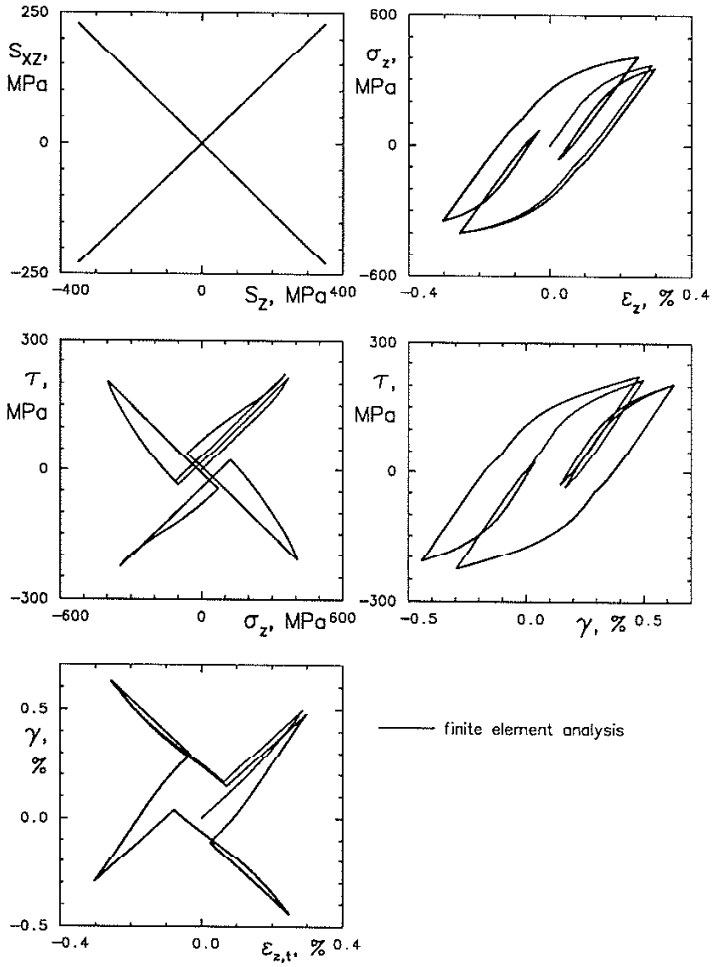

Figure 6: Non-proportional 'X' path loading of the mild notched round bar (finite element results)

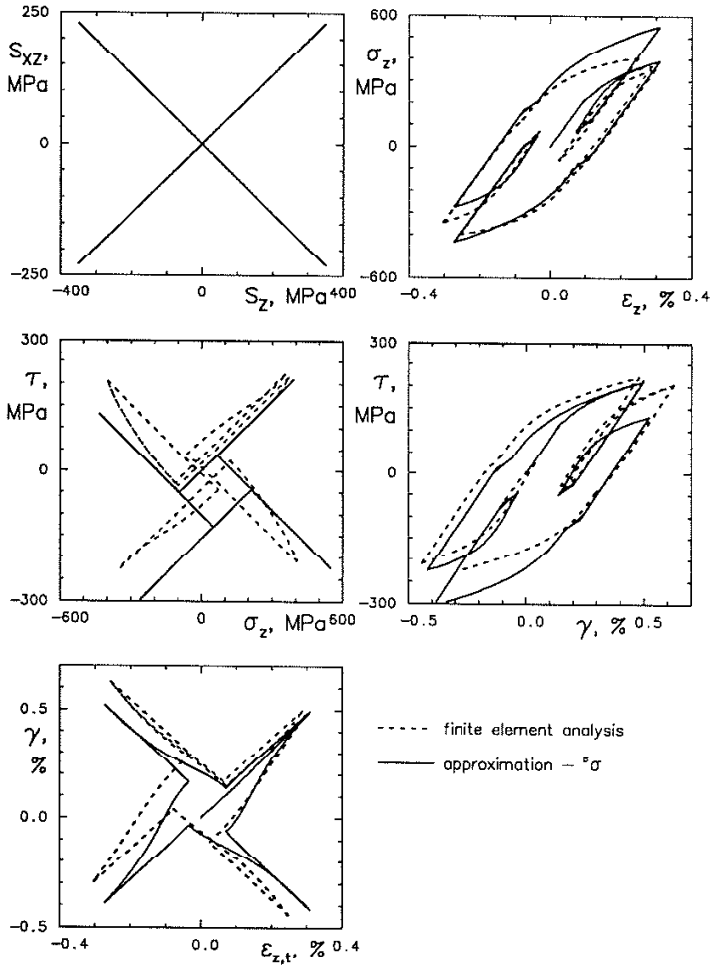

Figure 6: Non-proportional 'X' path loading of the mild notched round bar ($^e\sigma$ approximation)

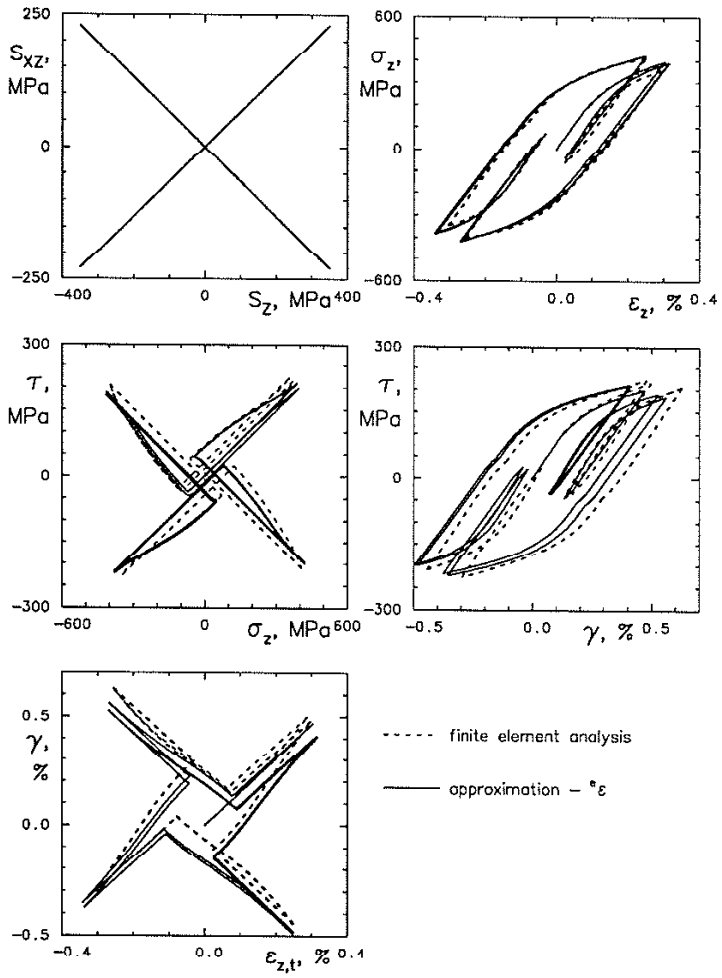

Figure 6: Non-proportional 'X' path loading of the mild notched round bar ($^e\varepsilon$ approximation)

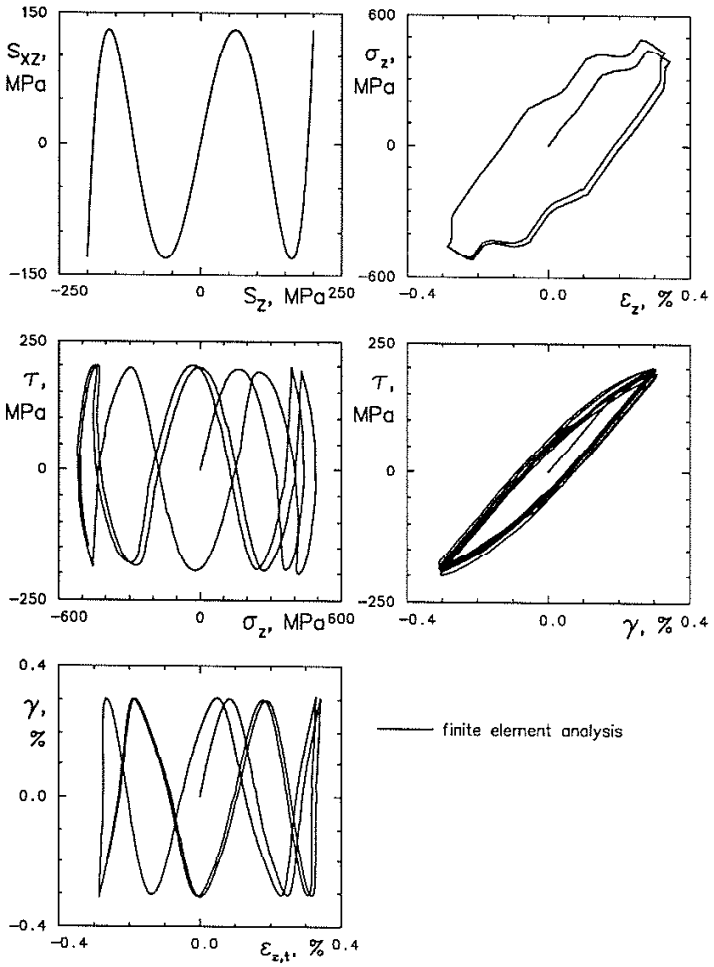

Figure 7: Sinusoidal loading with a frequency ratio of 1:5 of the sharp notched round bar (finite element results)

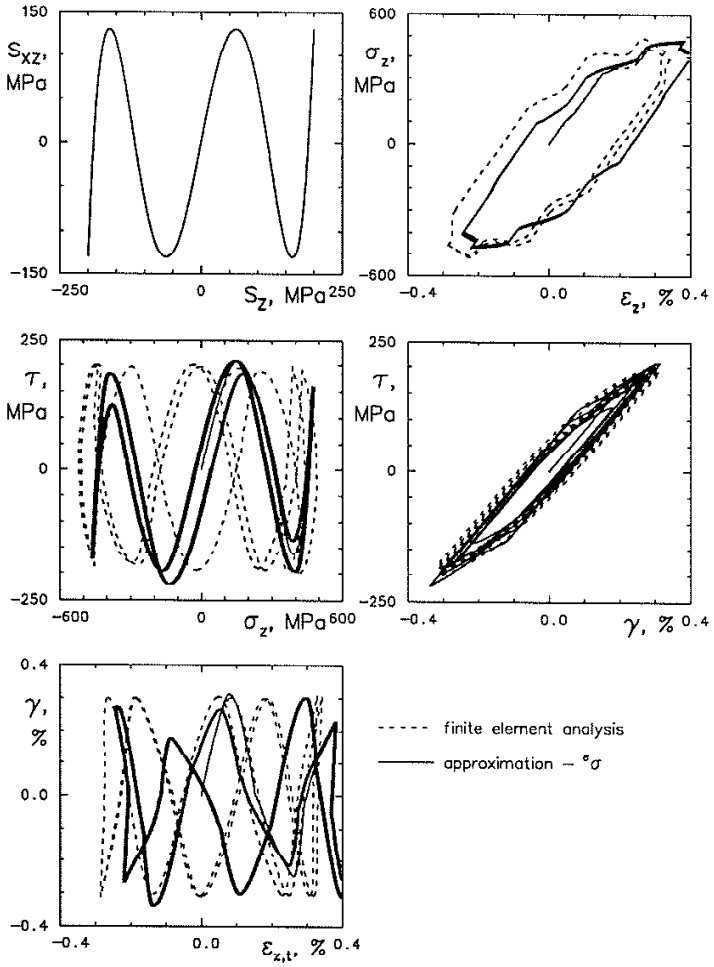

Figure 7: Sinusoidal loading with a frequency ratio of 1:5 of the sharp notched round bar ($^e\sigma$ approximation)

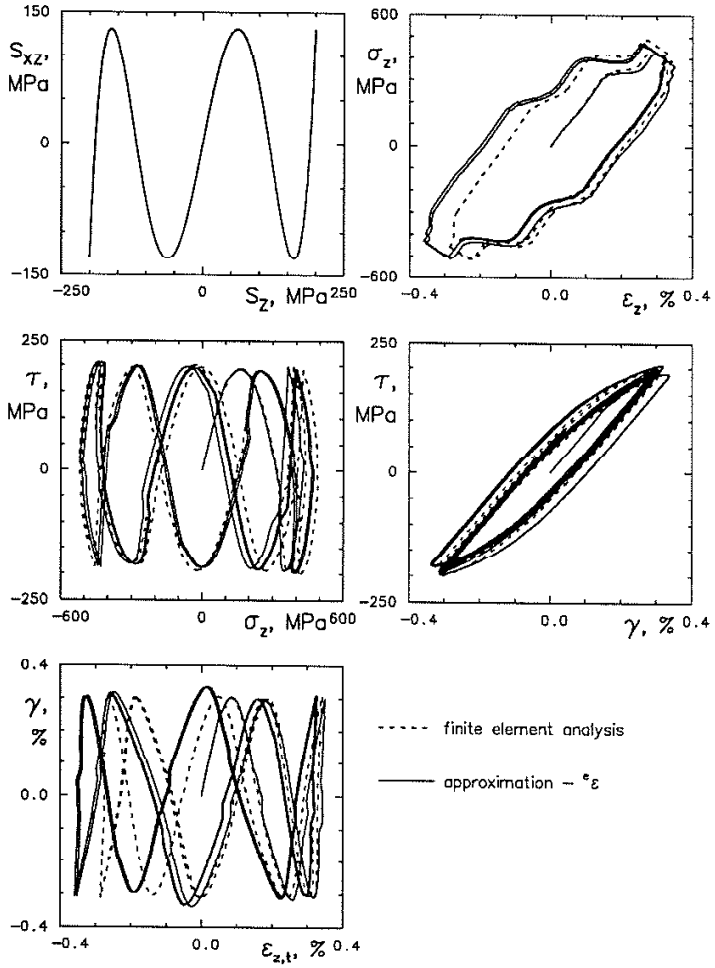

Figure 7: Sinusoidal loading with a frequency ratio of 1:5 of the sharp notched round bar ($^e\varepsilon$ approximation)

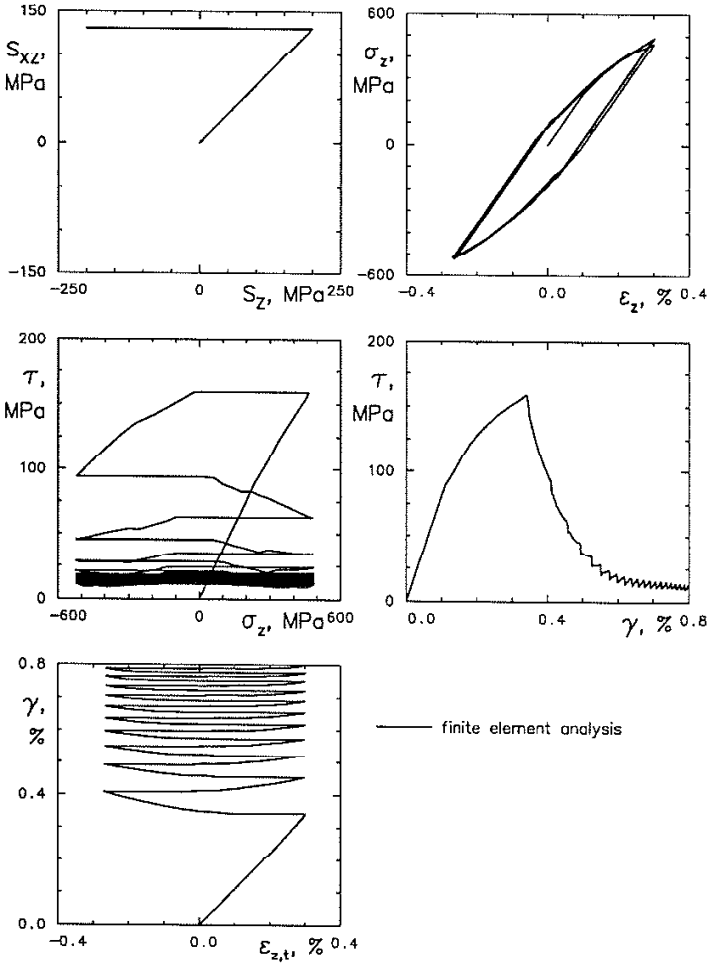

Figure 8: Constant torsional and fully reversed axial loading of the sharp notched bar (finite element results)

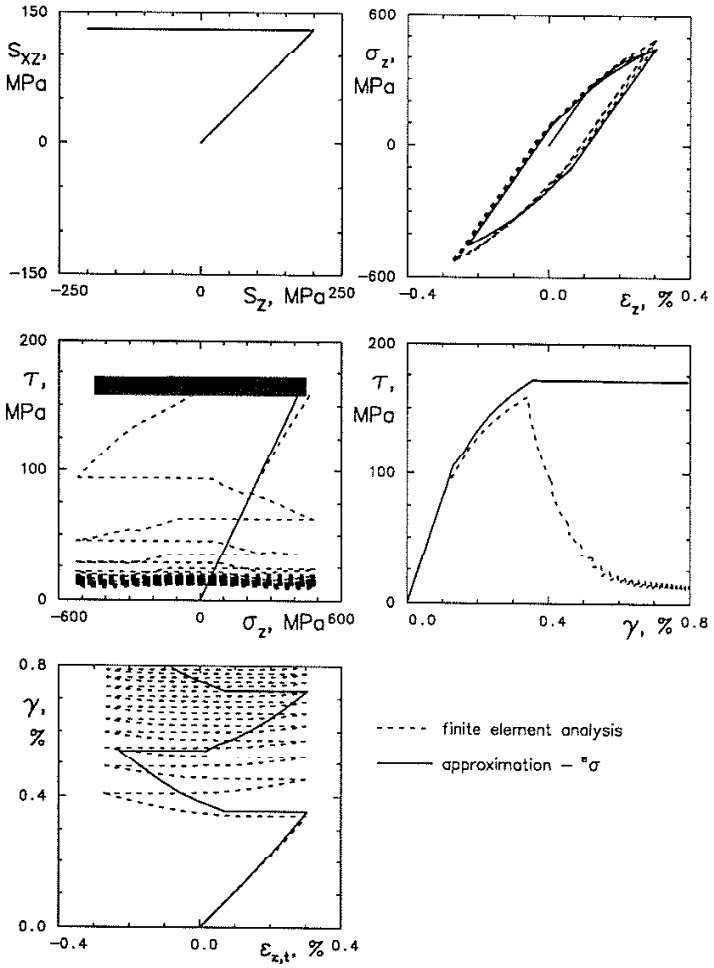

Figure 8: Constant torsional and fully reversed axial loading of the sharp notched bar ($^e\sigma$ approximation)

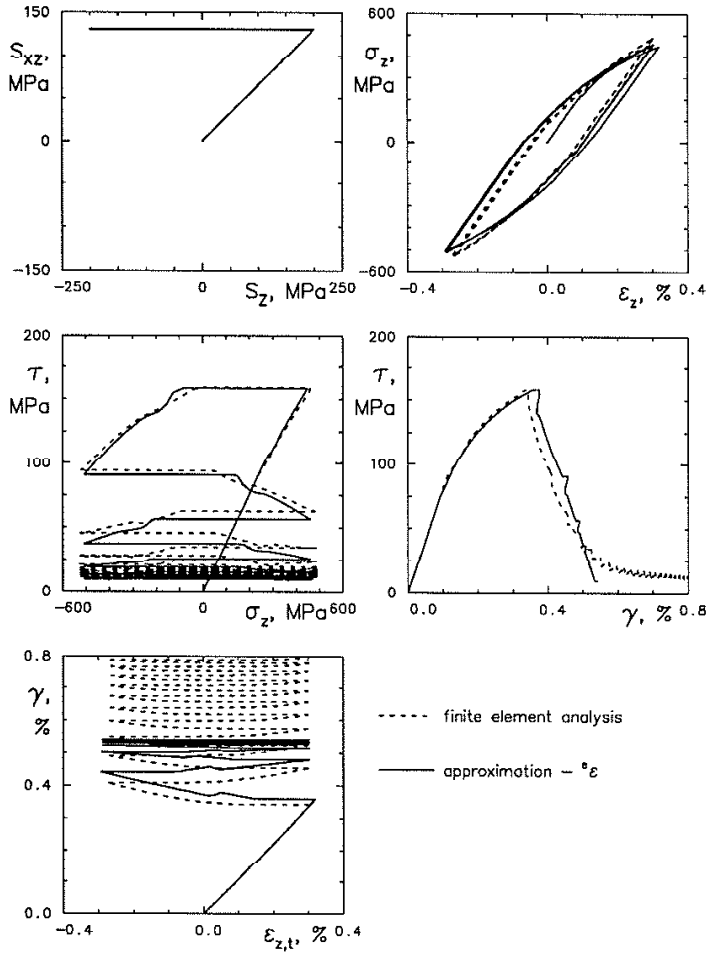

Figure 8: Constant torsional and fully reversed axial loading of the sharp notched bar ($^e\varepsilon$ approximation)